Published: 20 September 2026

Volume 13 | Issue 2 | 537-554

OPEN ACCESS

Journal of Daylighting

Journal homepage: www.solarlits.com/jd

RESEARCH ARTICLE

Integrated Multi-Metric Evaluation of Fixed External Shading Strategies and Window-To-Wall Ratio in a Hot–Dry, Clear-Sky Climate

Nima Jafarian Yazdi,[1] *Hadi Bagheri Sabzevar,*[1,*] *Mostafa Mohajerani*[2]

[1] *Department of Architectural Engineering, Hakim Sabzevari University, Sabzevar, Iran*

[2] *Department of Architecture and Urbanism, Shahrood University of Technology, Shahrood, Iran*

ABSTRACT

Daylighting-oriented façade design in hot–dry, clear-sky climates entails a fundamental trade-off between daylight availability and the mitigation of solar-driven thermal and energy penalties. This study proposes an integrated simulation-based framework to quantify the combined influence of the window-to-wall ratio (WWR) and fixed external shading strategies on daylight performance, annual energy demand, and thermal comfort in a south-facing office reference model in Mashhad, Iran. A standardized shoebox office model was evaluated under three WWR scenarios (30%, 50%, and 70%) and six fixed shading typologies—including planar systems (horizontal, three-sided, and four-sided overhangs, and a light shelf) and louver-based systems (horizontal louvers (H-louvers) and vertical louvers (V-louvers))—benchmarked against an unshaded baseline. Annual simulations jointly assessed spatial Daylight Autonomy (sDA), Useful Daylight Illuminance (UDI), Annual Sunlight Exposure (ASE), Energy Use Intensity (EUI), and Thermal Comfort Hours (TCH). Results for the unshaded baseline revealed that increasing the WWR from 30% to 70% predictably improved daylight sufficiency but severely compromised visual and thermal performance, driving the spatial ASE to 31.3% (failing LEED v4.1 limits) and decreasing thermal comfort hours by over 20%. Fixed external shading devices mitigated these adverse effects, with a critical tipping point identified at a 50% WWR. While planar shading systems maintain a viable balance below this threshold, their effectiveness sharply declines at higher glazing ratios. Through a parametric evaluation at the 50% WWR threshold, an optimized H-louver geometry (20 cm depth, 20 cm spacing) emerged as the most robust and highest-performing configuration. This configuration successfully satisfied LEED daylight criteria (ASE of 8.04%, sDA of 62%) while minimizing energy demand (EUI of 39 kWh/m^2·year) and maximizing thermal comfort (TCH of 1808 hours) among the evaluated configurations. Ultimately, the proposed framework demonstrates that complex performance trade-offs can be effectively resolved by matching specific shading geometries to precise glazing thresholds, providing actionable guidelines for solar-intensive environments.

Keywords: fixed external shading, climate-based daylighting, visual comfort, thermal comfort, energy performance, window-to-wall ratio

1. INTRODUCTION

Daylighting is widely recognized as a core component of high-performance building design due to its direct influence on visual comfort, occupant well-being, and building energy demand [1, 2]. Beyond reducing dependence on electric lighting, well-designed daylighting strategies enhance perceived indoor environmental quality, occupant satisfaction, and non-visual health outcomes,

*Corresponding author.

n.jafarian98@gmail.com (N. J. Yazdi); h.bagheri@hsu.ac.ir (H. B. Sabzevar. Mushtaha); m.mohajerani@shahroodut.ac.ir (M. Mohajerani)

Received 29 March 2026; Revised 5 August 2026; Accepted 9 August 2026; Published online 20 September 2026

Citation: Nima Jafarian Yazdi, Hadi Bagheri Sabzevar, Mostafa Mohajerani, Integrated multi-metric evaluation of fixed external shading strategies and window-to-wall ratio in a hot–dry, clear-sky climate, Journal of Daylighting, 13:2 (2026) 537-554. doi: 10.15627/jd.2026.30

NOMENCLATURE

ASE	*Annual Sunlight Exposure*
CBDM	*Climate-Based Daylight Modeling*
DF	*Daylight factor*
LEED	*Leadership in energy and environmental design*
Max	*Maximum*
Min	*Minimum*
PMV	*Predicted mean vote*
EUI	*Energy Use Intensity*
H-louver	*Horizontal louver*
sDA	*spatial Daylight Autonomy*
SHGC	*Solar Heat Gain Coefficient*
UDI	*Useful Daylight Illuminance*
V-louver	*Vertical louver*
WWR	*Window-to-Wall Ratio*
TCH	*Thermal Comfort Hours*

positioning daylight as a fundamental driver of sustainable building performance [3, 4]. However, daylighting is inherently a dual-natured parameter. While insufficient daylight reduces task performance and increases reliance on artificial lighting, excessive daylight—particularly uncontrolled direct solar radiation—results in glare, thermal discomfort, and elevated cooling energy demand [5, 6]. This intrinsic trade-off underscores the necessity of balancing daylight sufficiency and quality rather than merely maximizing its availability. Consequently, façade design decisions dictate whether daylight functions as a performance asset or a liability.

These challenges are particularly pronounced in hot–dry climates, where high solar intensity, clear-sky conditions, and extended periods of sunshine dominate the annual climatic profile [7, 8]. In such contexts, façade geometry and glazing characteristics exert a disproportionate influence on indoor environmental performance. Mashhad, Iran (ASHRAE climate zone 3B), exemplifies this condition with its high direct normal irradiance and pronounced seasonal temperature variations. Within this environment, the window-to-wall ratio (WWR) emerges as a critical parameter: increasing the WWR generally enhances spatial daylight penetration but simultaneously elevates solar heat gains, glare probability, and cooling demand, especially for south-facing façades exposed to sustained solar radiation [9, 10].

Historically, daylight performance assessment relied on static indicators such as the Daylight Factor (DF) [1]. While foundational, DF-based methods systematically underestimate the frequency and intensity of direct sunlight in clear-sky regions and fail to capture seasonal patterns of overexposure and glare [11, 12]. The emergence of Climate-Based Daylight Modeling (CBDM) marked a fundamental shift by utilizing hourly climatic data to evaluate both spatial and temporal daylight availability [13, 14]. This advancement supported the widespread adoption of dynamic metrics—now embedded in certification frameworks such as LEED v4.1 [15, 16]—including Spatial Daylight Autonomy (sDA) for daylight sufficiency, Useful Daylight Illuminance (UDI) to evaluate daylight quality by filtering out excessive illuminance, and Annual Sunlight Exposure (ASE) to target the spatial and temporal extent of direct sunlight as a proxy for glare risk [17]. Parallel developments in building energy simulation now allow these daylight metrics to be evaluated simultaneously alongside annual energy demand and thermal comfort, facilitating a truly multi-dimensional performance analysis [18].

Despite these advances, much of the existing literature continues to assess façade performance through fragmented or isolated metrics [13, 19]. Numerous studies report high sDA or UDI values without explicitly quantifying the associated overexposure risks (ASE), while others prioritize energy reduction without adequately addressing daylight distribution and visual comfort [20]. This fragmented approach is especially problematic in hot–dry climates, where the interactions between daylight availability, solar heat gains, and occupant comfort are strongly non-linear [13, 21]. Façade strategies that appear optimal under single-metric evaluations often exhibit counterproductive performance when assessed holistically.

Façade design variables, particularly WWR and external shading systems, act as critical mediators in these interactions. Planar shading devices, such as horizontal overhangs and light shelves, are commonly applied to south-facing façades to block high-angle solar radiation; however, their performance often degrades at higher WWR levels and during shoulder seasons [22]. Louver-based systems exhibit more complex behaviors. Horizontal louvers (H-louvers) provide continuous modulation of direct solar radiation across various solar angles and serve as robust solutions in cooling-dominated climates [13, 23, 24]. Vertical louvers (V-louvers), while effective for low-angle control, often reduce diffuse daylight penetration, leading to lower UDI values [25]. Similarly, optimal WWR ranges vary substantially depending on shading configuration, underscoring the inadequacy of universal design prescriptions [26, 27].

Therefore, this study evaluates how fixed external shading systems affect daylighting, energy demand, and thermal comfort in hot–dry climates. Specifically, it examines the interaction between different shading geometries and WWR to optimize the façade performance of a south-facing office.

2. BACKGROUND AND LITERATURE REVIEW

Early approaches to daylight performance assessment relied primarily on static indicators such as DF, which evaluates indoor illuminance under standardized overcast sky conditions [1]. While DF-based methods contributed to the development of early daylighting guidelines, they have been widely criticized for their inability to represent real climatic conditions, solar geometry, façade orientation, and temporal variability. These limitations are particularly evident in clear-sky regions, where DF systematically

https://dx.doi.org/10.15627/jd.2026.30

fails to capture direct sunlight's frequency and intensity, failing to account for seasonal patterns of overexposure and glare [11, 12].

The emergence of CBDM marked a fundamental shift in daylight performance evaluation by enabling the use of hourly climatic data to assess daylight availability and exposure across both space and time [14, 21]. Within this framework, sDA quantifies spatial daylight sufficiency, while UDI distinguishes between insufficient, useful, and excessive illuminance levels, providing a more nuanced assessment of daylight quality. ASE, in contrast, explicitly targets the spatial and temporal extent of excessive direct sunlight and has become a widely adopted proxy for overexposure and glare risk [17].

Despite these advances, individual CBDM metrics capture only partial aspects of indoor visual conditions. High sDA values may coincide with elevated ASE, indicating that spatial daylight sufficiency is achieved at the expense of increased visual discomfort. Conversely, low ASE values may obscure inadequate daylight penetration, leading to increased reliance on electric lighting despite apparent solar control [19]. Although UDI partially bridges this gap by accounting for excessive illuminance, it does not explicitly address spatial sufficiency or the thermal implications associated with solar gains [28]. Furthermore, these thermal outcomes are deeply influenced by dynamic occupant behaviors; for instance, probabilistic window-opening strategies can substantially alter adaptive thermal comfort across different climatic and seasonal conditions [29]. Consequently, recent daylight research increasingly emphasizes the need to interpret sDA, UDI, and ASE collectively within integrated assessment frameworks rather than as isolated indicators [13].

Façade design variables, particularly WWR and external shading systems, play a decisive role in shaping these interactions. Increasing WWR generally enhances daylight penetration and spatial sufficiency but simultaneously amplifies solar heat gains, glare probability, and cooling demand, especially in solar-intensive climates [9, 10]. External shading devices, therefore, function as critical mediators between daylight availability and solar control, influencing how daylight metrics translate into actual visual, thermal, and energy performance outcomes.

Previous studies have evaluated various shading configurations, highlighting their influence on daylight distribution, glare mitigation, and energy performance [30, 31]. Planar shading devices, such as horizontal overhangs and light shelves, are commonly applied to south-facing façades due to their effectiveness in blocking high-angle solar radiation. However, several studies report that their performance degrades at higher WWR levels and during shoulder seasons, particularly in clear-sky climates where solar altitude and azimuth vary significantly throughout the year [22].

Louver-based systems exhibit more complex performance characteristics. H-louvers provide consistent interception of direct solar radiation across a wide range of solar angles and have been identified as relatively robust solutions for balancing daylight availability, glare control, and energy performance in cooling-dominated climates [13, 23, 24]. V-louvers, while effective for low-angle solar control, often reduce diffuse daylight penetration, resulting in lower UDI values despite improved glare mitigation [25].

Parallel research on WWR consistently demonstrates its strong influence on both daylight and energy outcomes. While higher WWR values enhance daylight sufficiency, they are also associated with increased solar heat gains, thermal discomfort, and cooling energy demand in hot–dry climates [26]. Consequently, reported optimal WWR ranges vary substantially depending on shading configuration, façade orientation, and climatic context, underscoring the need for case-specific, multi-performance evaluation rather than universal design prescriptions [27].

2.1. Research gap and contribution

Despite extensive research on daylighting, façade design, and external shading systems, several critical limitations remain unresolved in the current literature. First, although CBDM has become the dominant paradigm, and recent multi-objective optimization studies have advanced the field by simultaneously evaluating metrics like sDA and EUI (Energy Use Intensity), they frequently present abstract Pareto fronts that lack prescriptive clarity for designers. Moreover, many of these multi-metric approaches treat performance variables as linear trade-offs, failing to capture the sudden, non-linear tipping points of overexposure (ASE) and thermal discomfort that occur under extreme direct irradiance. Consequently, even among integrated studies, there is a lack of evaluation frameworks that translate complex multi-objective data into concrete, threshold-based architectural guidelines.

Second, while both WWR and shading geometry are widely recognized as key façade variables, their interactive effects are frequently investigated in isolation. Numerous studies assess individual shading typologies at a single glazing ratio, whereas others explore WWR optimization without systematically accounting for shading configuration. This fragmented treatment limits the ability to derive robust design guidance, as façade strategies that perform well at one WWR may exhibit substantially different behavior at higher or lower glazing ratios.

Third, hot–dry, clear-sky climates remain underrepresented in integrated multi-performance façade studies. In such climates, high solar intensity and prolonged direct sunlight fundamentally alter the balance between daylight benefits and thermal penalties, amplifying trade-offs between daylight availability, glare probability, and cooling demand. Findings derived from temperate or mixed climates, therefore, cannot be directly extrapolated to hot–dry regions without risking misleading conclusions, particularly for south-facing office façades subject to sustained annual solar exposure. A comprehensive summary of these previous studies, highlighting their geographical contexts, evaluated parameters, and multi-performance criteria, is provided in **Table 1**.

Table 1. Lighting in educational buildings, study areas, assessment standards, and adopted methodologies as presented in previous works of literature.

Authors (Year)	Title	Climate / Location	Building Type	Shading System	WWR Considered	Daylight Metrics
[20]	Automatic evaluation and analysis of indoor visual comfort for sustainable building design using interpretable ensemble learning	Tropical Dry Temperate Continental Polar climates	Office	Building form (Dimension) window (WWR, Height and sill Height and transmittance) Shading Device (Length and angle) Surface material (Reflectance of inner surface)	-	UDI, ASE, GA, sGA
[13]	Multi-objective optimization of energy, thermal and visual comfort for dormitory buildings in the cold climate of China	Cold climate	University dormitory	External louvers + envelope & roof variables (incl. green roof) WWR	-	UDI, DA
[32]	Daylight Optimization in Tropical Architecture: A LEED v4-Based Case Study of a Hypothetical Office Building in Chittagong, Bangladesh	Tropical hot–humid	Office	Overhangs (south façade) V-louvers (east/west façades)	-	sDA ASE
[33]	Daylight Availability of Living Rooms in Dense Residential Areas under Current Planning Regulations: A Cross-Region Case Study in China	Four local daylight climate zones (Kunming, Tianjin, Changsha, and Chongqing cities)	Residential	Urban form and planning regulations	-	DF, sDA, UDI, m-EDI (circadian metric)
[34]	Evaluating Annual Sun Exposure in LEED v4 for Commercial Office Buildings: Inclusion of Annual Glare to Enhance Occupant Visual Performance and Comfort	Temperate	Office	Overhang and Interior louvers (comparative scenarios)	-	ASE sDA DGP
[35]	Multi-performance Optimization of Static Shading Devices for Glare, Daylight, View and Energy Consideration	Cold climate	Educational (classrooms)	Fixed external shading devices overhang with fins H-louvers v-louvers, eggcrate light shelf	-	sDA cDA UDI
[36]	Optimizing daylight, energy and occupant comfort performance of classrooms with photovoltaic-integrated vertical shading devices	Hot–dry	Educational (classroom)	Fixed v-louvers with photovoltaic-integrated shading devices parametric forms	-	UDI ASE DGP
[37]	A novel method for simulating dynamic facades to analyze and optimize daylight and visual comfort in office buildings. Opt Facades for Daylight and Visual Comfort	Hot–arid climate	Office	Dynamic external H-louvers	-	UDI DGP
[19]	A study on daylighting metrics related to the subjective evaluation of daylight and visual comfort of students in China	Subtropical climate	Educational (school classrooms)	A study on daylighting metrics	-	sDA DA UDI ASE sDG DFavg
[38]	Daylight Comfort Performance of a Vertical Fin Shading System: Annual Simulation and Experimental Testing of a Prototype	Temperate climate	Office (south-facing test room)	Vertical fin shading system	-	UDI Illuminance DGP ASE
[15]	Daylighting performance evaluation in tropical lecture rooms: A comparative analysis of static and climate-based metrics	Tropical	Educational (university lecture rooms)	Existing static shading systems (vertical shading Bilateral louver Coved terrace eggcrate shading)	-	Effective daylight ratio DA sDA UDI

https://dx.doi.org/10.15627/jd.2026.30

[39]	Design Adjustments for Daylighting and Visual Comfort in a Classroom with Conventional Shadings	Temperate climate	Educational (university classroom)	Roller shades and internal louvers with design adjustments (clear upper glazing vs full coverage)	-	UDI Uniformity sDG View Factors
[23]	Evolving multi-objective optimization framework for early-stage building design: Improving energy efficiency, daylighting, view quality, and thermal comfort	Hot-Humid Warm-Humid Mixed-Humid Cool-Dry Cold-Humid	Office	Form Geometry (aspect ratio, orientation) WWR Shading Devices Fabric roller blinds (dynamic operation considered within optimization framework)	Yes, treated as a key design variable (parametric across scenarios	UDI sDA DA cDA
[40]	Influence of Sun Shading Devices on Energy Efficiency, Thermal Comfort and Lighting Comfort in a Warm Semi-Arid Dry Mediterranean Climate	Warm semi-arid dry Mediterranean	Educational (university classrooms)	Movable sun shading devices: vertical exterior louvers indoor venetian blinds outdoor venetian blinds	-	Illuminance levels lighting comfort indicators
[27]	Maximize Energy Efficiency in Homes: A Parametric Simulation Study Across Chile	Desert with cloud cover, cold desert, standard desert, warm-temperate warm-summer Mediterranean, highland tundra, oceanic, subpolar oceanic.	Residential	39 Passive strategies including overhangs, façade-related measures and WWR	-	
[41]	Multi-objective optimization for high-performance building facade design: A systematic literature review	Temperate / East Asia (case-study based)	Office building	External shading devices integrated with façade and fenestration design variables	Yes, treated as a parametric design variable	sDA, UDI, DA
[42]	Multi-objective optimization of energy, view, daylight and thermal comfort for a building's fenestration and shading system in hot-humid climates	Hot–humid climate	Office	Shading devices dimensions WWR	-	sDA UDI SDA ASE
[43]	Multi-dimensional optimization for optimum modifications of light-shelves parameters for daylighting and energy efficiency	Tropical climate	Office workspace	Light-shelf system (external + internal configurations, parametric geometry)	-	sDA UDI
[26]	Optimization of energy consumption and daylight performance in residential building regarding windows design in hot and dry climate of Isfahan	hot and dry climate	Residential	Window angle relative to the edges of the wall	-	DF, UDI
[44]	Optimum external shading system for counterbalancing glare probability and daylight illuminance in Sydney's residential buildings	Humid subtropical	Residential	Fixed external shading devices (rectangular and tapered polygonal shades; optimized geometry) WWR	-	UDI DGP sDG Ev
[45]	Performance Assessment of Light Shelves System in Office Building	Cold semi-arid (BSk)	Office	Light shelves (external, internal, hybrid and angle configurations) WWR	Yes, 60%, 70%, 80%, 90%	UDI DF DGP
[46]	Performance analysis of light shelves in providing visual and thermal comfort and energy savings in residential buildings	Hot–dry / Mashhad, Iran	Residential	Light shelves (horizontal and vertical; internal configurations)	-	Illuminance
[47]	Ten Questions Concerning Environmental Architectural Design Exploration	Multi-climate / conceptual & multi-case synthesis	Various (methodological framework)	Not specific (design exploration framework including façade and shading parameters)	Yes (as a key design parameter in the framework	sDA, UDI, ASE (framework-level discussion)

[48]	The impact of facade geometry on visual comfort and energy consumption in an office building in different climates	cold semi-arid hot semi-arid moist mild-latitude cold semi-arid	Office	WWR window shape glazing material self-shading geometry	-	sDA UDI ASE
[23]	Evolving a multi-objective optimization framework for early-stage building design: Improving energy efficiency, daylighting, and view quality, and thermal comfort	Hot-Humid Warm-Humid Mixed-Humid Cool-Dry Cold-Humid	Office	Aspect ratios Orientation WWR Shading variable (Number and size) Windows Construction Fabric blind construction	-	Illuminance UDI
[49]	Daylighting Performance and Thermal Comfort Performance Analysis of West-Facing External Shading for School Office Buildings in Cold and Severe Cold Regions of China	Cold & severe cold climates	Office (University buildings)	H-louver & V-louver (Number, Width and Angle of Slats) Distance between shade and windows horizontal & Vertical Baffle (Width and Angle)	-	UDI
[24]	Evaluation of Daylighting Performance, Glare Control, and Thermal Comfort Using Light Shelves and Internal Louvers in Office Buildings	hot-arid climate	Open-plan office	Light shelves (internal / external / intermediate) + internal louvers	Yes, 30%, 50%, 70%	UDI, sDA, ASE, sGA, SVD

To address these critical gaps, this study systematically evaluates six fixed external shading typologies—horizontal overhangs, three-sided overhangs, four-sided overhangs (eggcrates), H-louvers, V-louvers, and light shelves—across three representative WWR scenarios (30%, 50%, 70%) for a south-facing office in a hot–dry, clear-sky climate (Mashhad, Iran; ASHRAE Zone 3B). By integrating CBDM-based daylight metrics (sDA, UDI, ASE) with annual energy demand (EUI) and PMV (Predicted Mean Vote)-based thermal comfort assessment within a unified simulation framework, this study provides a multi-dimensional comparison of façade strategies. The genuine novelty of this work lies not merely in conducting a multi-metric simulation, but in identifying specific, non-linear performance boundaries where different fixed shading strategies transition from beneficial to detrimental as the WWR increases. By pinpointing these precise tipping points—where the benefits of daylight sufficiency are precipitously overwhelmed by thermal and visual penalties—this study translates complex performance data into robust, evidence-based thresholds, thereby refining general façade design heuristics for extremely sunny, hot–dry environments.

3. METHODOLOGY

This study adopts an integrated, simulation-driven parametric framework to evaluate the multi-performance behavior of fixed external shading systems in office buildings across multiple WWR scenarios. The methodological workflow comprises: (i) climatic characterization of the study location; (ii) development of a standardized reference office model; (iii) definition of WWR scenarios and fixed shading typologies; (iv) annual performance evaluation across daylight, energy, and thermal comfort dimensions; and (v) integrated multi-performance assessment aligned with internationally recognized criteria, including LEED (**Figure 1**).

3.1. Climate characterization

The reference building is located in Mashhad, Iran (36.24° N, 59.63° E, Elevation: 999 m, classified as ASHRAE climate zone 3B (hot–dry). Simulations were conducted using a Typical Meteorological Year (TMY2) weather file for Mashhad, which is a composite of typical months selected from the historical period of 1999 to 2017. The climate is characterized by predominantly clear skies (> 65% annual probability) and high solar radiation (Global Horizontal Irradiance ≈ 1750 kWh/m^2, Diffuse horizontal irradiance ≈ 550 kWh/m^2). Significant thermal fluctuations occur throughout the year, with summer temperatures frequently exceeding 35 °C and winter temperatures occasionally falling below -20 °C. These conditions underscore the critical need for effective façade design to balance daylighting and mitigate solar overheating.

3.2. Base reference model (shoebox model)

A simplified single-zone shoebox office model, originally proposed by Reinhart [50], was adopted due to its suitability for façade-focused parametric investigations and its widespread use in comparative daylighting studies. The model has a depth of 6.00m, a width of 4.00m, and a height of 3.00m, featuring a single south-facing window defined by a sill height of 0.80m and a head height of 2.40m.

To isolate façade-driven effects, all interior surfaces except the south façade were modeled as adiabatic. This assumption eliminates confounding inter-zonal heat transfer, ensuring that the observed variations in daylight, energy, and thermal comfort performance are attributable exclusively to changes in the glazing ratio and external shading configurations.

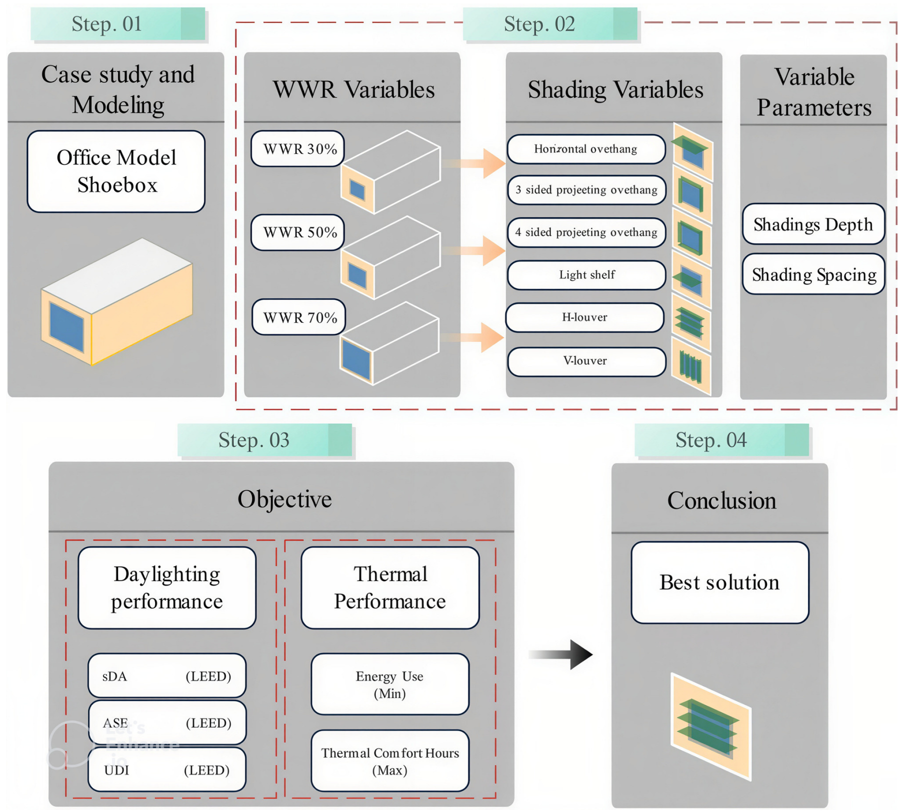

Figure 1. Overview of the integrated simulation-based methodological framework used to assess fixed external shading typologies across multiple WWR scenarios.

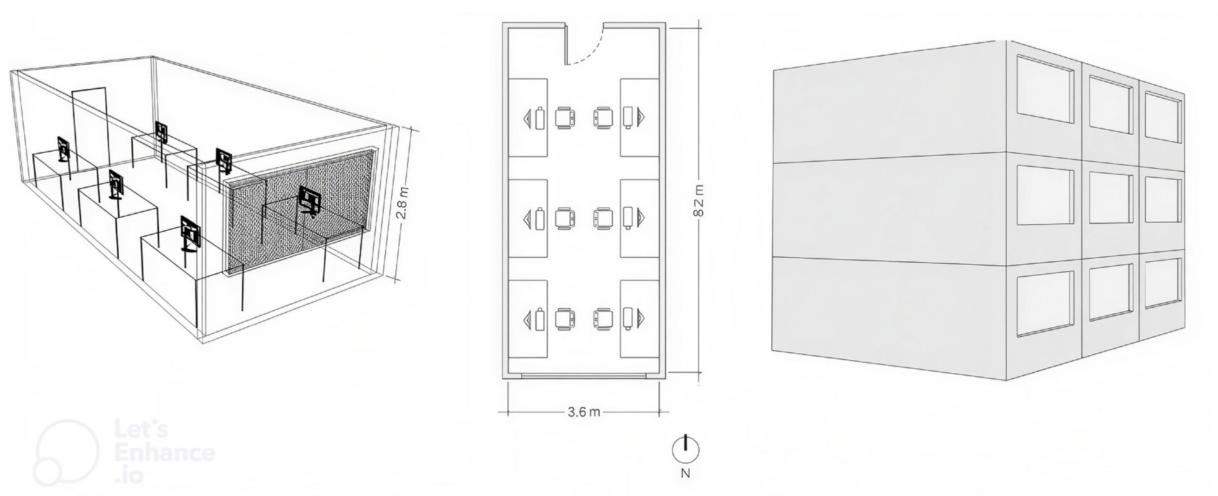

Figure 2. Perspective and plan of the reference office model [51].

Figure 2 illustrates the perspective view and floor plan of the reference office model adopted in this study.

3.3. Research scenarios

Three WWR scenarios (30%, 50%, and 70%) were selected to represent low, moderate, and high glazing conditions commonly observed in contemporary office façades. This parametric range is essential to effectively capture non-linear transitions in building performance. Furthermore, although a 70% WWR is generally not recommended for hot–dry climates, it was intentionally included as an extreme boundary condition to evaluate severe performance degradation and test the maximum limits of the proposed shading strategies. Across all scenarios, the window sill height was maintained at 0.800m, while the window width and height were adjusted to achieve the target WWR levels. This approach ensured geometric consistency and enabled the direct attribution of performance variations to changes in the glazing ratio alone. The resulting configurations are illustrated in Figure 3.

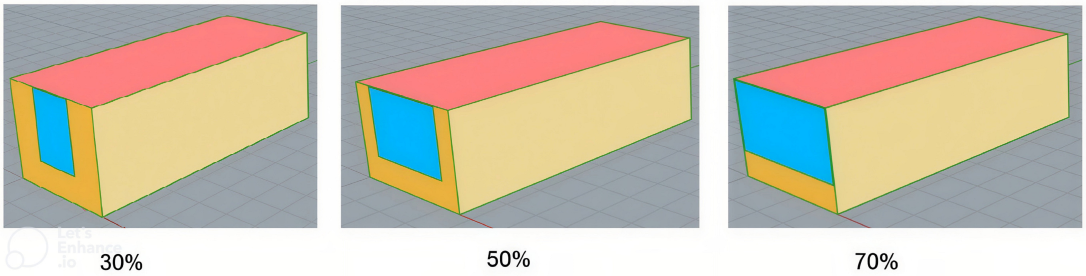

Figure 3. Reference office model configurations corresponding to WWR of 30%, 50%, and 70%.

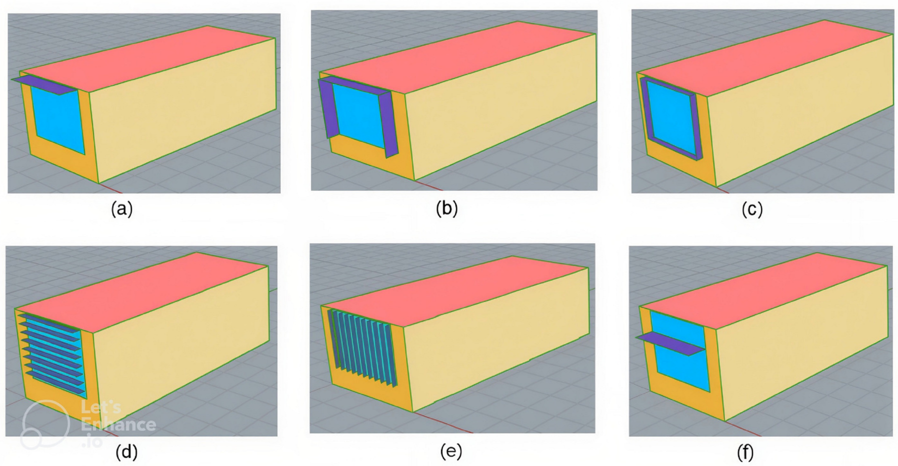

Figure 4. Representative geometrical configurations of the investigated fixed external shading typologies. (a): Horizontal overhang, (b): 3-sided projecting overhang, (c) 4-sided projecting overhang, (d) H-louver, (e) V-louver, (f) Light shelf.

3.4. External shading typologies and parametric definition

Six fixed external shading typologies were investigated: (i) horizontal overhang, (ii) three-sided overhang, (iii) four-sided overhang (eggcrate), (iv) H-louvers, (v) V-louvers, and (vi) light shelf. A baseline configuration without external shading was included for reference. The geometric parameters of each shading typology were systematically varied within ranges reported in validated parametric studies. For projecting shading devices, depth was considered the primary control parameter. For louver-based systems, both depth and spacing were varied to capture directional solar modulation effects. For light shelves, interior and exterior depths were independently adjusted to reflect their combined solar control and daylight redirection functions. The investigated parameter ranges are summarized in Table 2, and representative geometries are illustrated in Figure 4. A total of 234 annual simulation scenarios were constructed by combining three WWR levels with six fixed shading typologies, in addition to three baseline no-shading cases.

3.5. Simulation setup and parameters

All simulation workflows were executed within the Rhinoceros/Grasshopper environment utilizing the Ladybug Tools plugin (Version 1.5, including Honeybee). Annual daylight performance was evaluated using a CBDM approach driven by the Radiance engine. Performance was quantified using sDA300/50%, ASE1000/250h, and the mean spatial UDI300-3000, in accordance with IES LM-83-12 definitions and LEED criteria. The reported UDI is the spatial average of the values calculated at each individual sensor across the floorplan. All daylight simulation parameters, including surface reflectance values, glazing visible transmittance, work plane height, sensor grid resolution, and occupancy schedule, were held constant across all scenarios to ensure comparability. The adopted parameters are summarized in Table 3.

Thermal and energy performance were evaluated using annual dynamic simulations powered by the EnergyPlus engine. A simulation timestep of 6 was selected to accurately capture the dynamic thermal interactions between the building envelope, solar shading, and internal heat gains. An Ideal Loads Air System was employed to isolate envelope-driven effects and avoid confounding influences associated with HVAC system efficiencies. Performance indicators included annual heating load, cooling load, and EUI. Construction assemblies, glazing properties, and thermal boundary conditions were defined based on materials commonly used in Iranian office buildings. Heating and cooling setpoints followed national guidelines. Detailed material properties and thermal settings are provided in Table 3.

Table 2. Parameter ranges for fixed external shading devices.

Shading Device Type	Variable Parameters Range (cm)	Step	Number of Scenarios (Across 3 WWRs)
Horizontal (overhang)	Depth: 10-100	10	30
Three-sided overhang	Depth: 10-40	10	12
Four-sided overhang	Depth: 10-40	10	12
H-louver	Depth: 10-40	10	60
	Spacing: 5-25	5	
V-louver	Depth: 10-40	10	60
	Spacing: 5-25	5	
Light shelf	Depth (Ext): 20-80	20	60
	Depth (Int): 10-50	10	

Table 3. Key parameters for daylight, thermal, and energy simulations.

Constant daylight parameters:		**Value**		
Simulation period		One year		
Occupancy hours		8:00–18:00 (excluding Thursday and Friday)		
Floor reflectance		20%		
Wall reflectance		50%		
Ceiling reflectance		70%		
Shading reflectance		30% (For materials such as exposed concrete, fiber cement panels, or dark anodized aluminum)		
Visible transmittance of glazing (VT)		0.88		
Work plane height		80 cm		
Analysis grid spacing		50 cm		
Opaque wall construction layers and thermal properties				
Layers (outside to inside)	**Thermal Conductivity (W/m·K)**	**Specific Heat (J/kg·K)**	**Density (kg/m³)**	**Thickness (cm)**
Travertine Stone	1.4	950	2000	2
Mortar	0.72	700	1860	3
AAC Block (Autoclaved Aerated Concrete)	0.17	1000	700	20
Gypsum plaster	0.4	1000	1000	3
Window thermal and optical properties				
Property			**Value**	
U-factor (W/m²·K)			5	
Solar heat gain coefficient (SHGC)			0.78	
simulation settings				
Constant Variable			**Value**	
Simulation period			One year	
Heating setpoint [52]			20 °C	
Cooling setpoint [52]			28 °C	

Thermal comfort was evaluated using Fanger's PMV model. Thermal Comfort Hours (TCH) was defined as the occupied hours during which PMV values fell within the acceptable range of -0.5 to +0.5. To focus on façade-related effects, air velocity, metabolic rate, and seasonal clothing insulation were held constant across all simulations. The parameters used were: airspeed at 0.1 m/s, an activity level of 1.1 met, summer clothing insulation at 0.5 clo, and winter clothing insulation at 1.0 clo.

3.6. Model setup and consistency checks

Since this study employs a generalized parametric shoebox model rather than replicating a specific existing building, an empirical validation against measured field data was not applicable. Instead, model reliability was established through rigorous consistency checks and an analytical validation approach. The daylight and energy simulations were performed using Radiance and EnergyPlus, respectively.

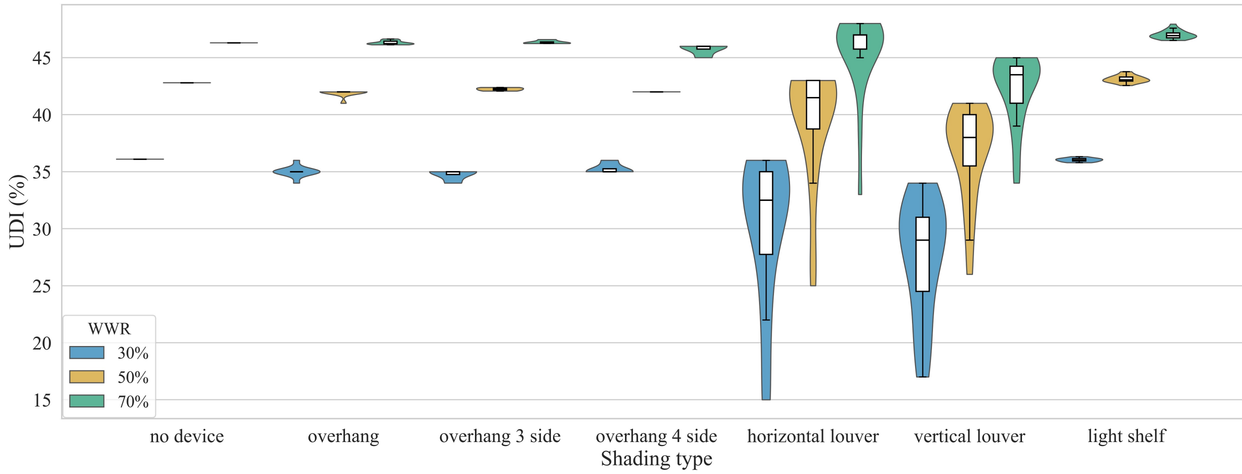

Figure 5. UDI index for various types of shadings.

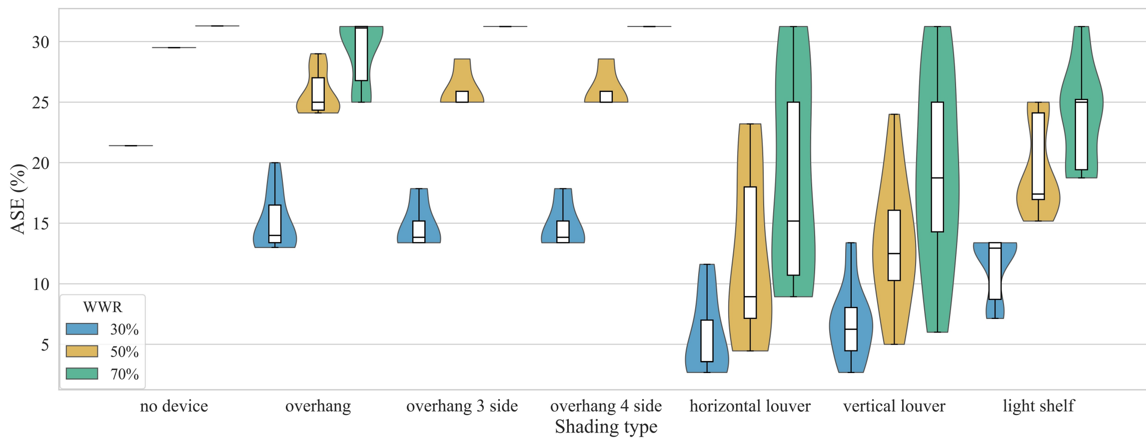

Figure 6. ASE index for various types of shadings.

Both are globally recognized engines that have been extensively tested, with EnergyPlus analytically validated against the ASHRAE Standard 140 protocol. To ensure consistency and procedural accuracy, all simulation inputs were strictly aligned with established standards: daylight simulation settings followed IES LM-83 recommendations, energy models were configured in line with ASHRAE 90.1 assumptions, and the shoebox geometry was verified according to Reinhart's guidelines. Material properties were benchmarked against validated literature values to ensure representativeness. Furthermore, the comprehensive brute-force parametric method inherently acted as an extensive consistency check across all simulated scenarios.

3.7. Multi-performance evaluation framework

Façade performance was evaluated across four complementary dimensions using standardized thresholds: daylight sufficiency and quality (sDA, UDI), overexposure risk (ASE1000/250h), thermal comfort availability (TCH per ASHRAE-55), and total energy performance (EUI). To systematically compare shading–WWR combinations under hot–dry, clear-sky conditions and assess parametric sensitivity, an exhaustive brute-force search was conducted utilizing the Colibri component in Grasshopper. By simulating all discrete design permutations, this framework maps the entire performance landscape. This comprehensive mapping inherently serves as a sensitivity analysis, explicitly quantifying how variations in individual geometric parameters impact the outputs. Consequently, this approach enables consistent cross-comparative analysis and the identification of multi-objective trade-offs, rather than optimizing individual metrics in isolation.

4. RESULTS

A total of 234 parametric shading simulation runs (excluding the unshaded baseline scenarios) were executed, with the precise number of configurations for each shading typology detailed in Table 2. Figure 5 illustrates the comprehensive distribution of UDI for the unshaded baseline alongside the six external shading typologies. The violin–box plots encompass all parametric variants—accounting for distinct WWRs, depths, and spacings—to capture the full performance spectrum within the optimal useful daylight threshold.

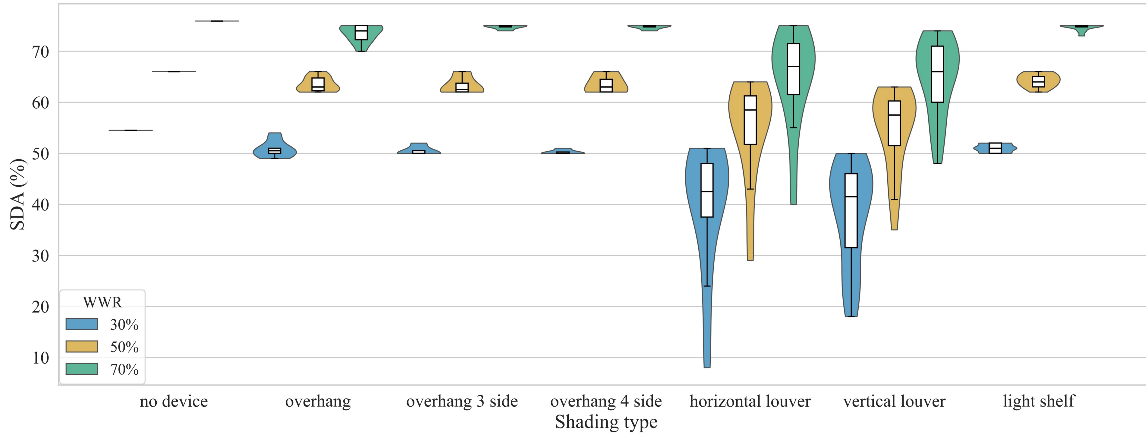

Figure 7. SDA index for different types of shadings.

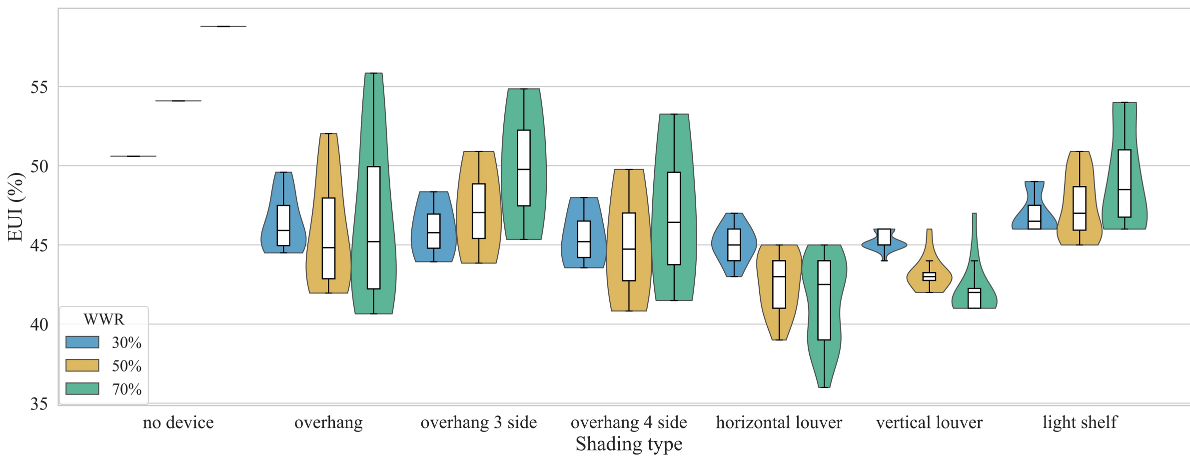

Figure 8. Energy consumption for various types of shadings.

UDI: Across all façade configurations, UDI demonstrates a pronounced dependence on WWR. At a 30% WWR, the median UDI for the baseline condition is 36.10%, while overhang-based typologies yield comparable median values converging around 35.00%. These relatively low percentages reflect the inherent limitation of useful daylight availability at restricted glazing ratios. In contrast, slatted shading systems (H-louvers and V-louvers) exhibit lower median values (32.50% and 29.00%, respectively) accompanied by substantially wider interquartile ranges, underscoring their heightened geometric sensitivity and the elevated risk of over-shading at reduced window areas.

Expanding the WWR to 50% yields systematic improvements in UDI across all configurations, characterized by concurrent reductions in performance variability. Under this moderate glazing scenario, the baseline median reaches 42.80%, with standard overhangs closely tracking at 42.00%. Notably, H-louvers and V-louvers experience significant performance recoveries, achieving medians of 41.50% and 38.00%, respectively. This indicates that a balanced glazing ratio optimizes both the penetration and spatial stability of functional daylight.

At the maximum simulated WWR of 70%, median UDI values peak across all evaluated cases. The baseline achieves 46.30%, while H-louvers and light shelves record the highest programmatic performances at 47.00% and 46.94%, respectively. However, for the unshaded baseline and standard overhangs, increasing WWR from 50% to 70% yields only marginal performance gains relative to the substantial expansion in glazing area. This plateau signifies a threshold of diminishing returns, where the proportional increase in useful daylight is increasingly counteracted by episodes of excessive, glaring illuminance.

Among all evaluated typologies, the light shelf consistently demonstrates the highest robustness. It maintains elevated and tightly clustered UDI distributions across all scenarios, ascending steadily from a median of 36.03% at WWR 30%, to 43.06% at WWR 50%, and culminating at 46.94% at WWR 70%. Ultimately, these findings corroborate that while increasing the WWR generally augments raw daylight availability, the implementation and specific typology of shading devices remain the critical determinants in stabilizing daylight autonomy and mitigating extreme illuminance variability, particularly within highly glazed environments.

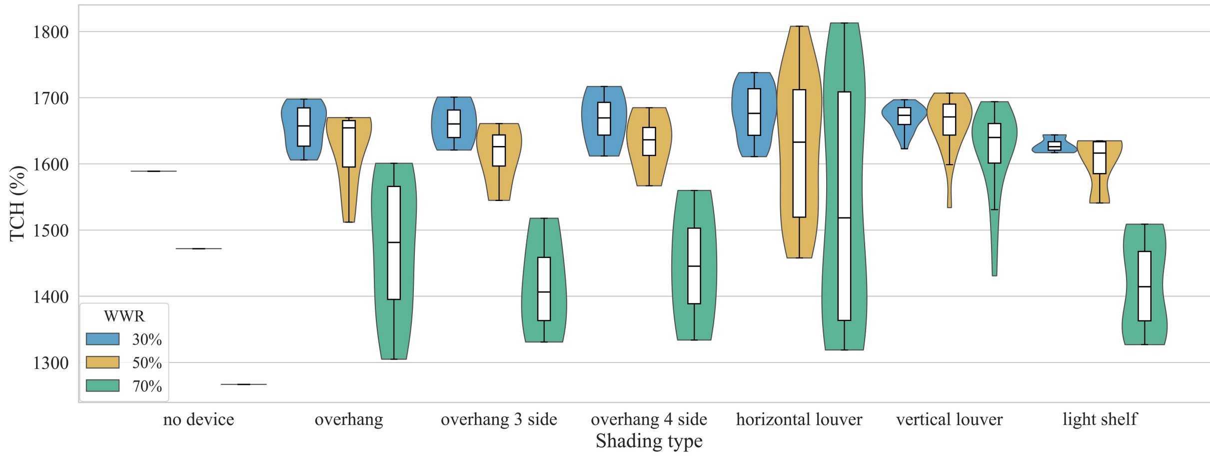

Figure 9. Total TCH index for various types of shadings.

Table 4. Median performance indicators of fixed shading typologies across WWR scenarios.

Shading typology	sDA (%) (30/50/70)	UDI (%) (30/50/70)	ASE (%) (30/50/70)	EUI (kWh/m²·year) (30/50/70)	TCH (h) (30/50/70)
H-louvers	42.5 / 58.5 / 67.0	32.5 / 41.5 / 47.0	3.6 / 8.9 / 15.2	45.0 / 43.0 / 42.5	1676.5 / 1633.0 / 1518.5
Light shelf	51.0 / 64.0 / 75.0	36.0 / 43.1 / 46.9	12.9 / 17.4 / 25.0	46.5 / 47.0 / 48.5	1626.0 / 1616.5 / 1414.5
No device	54.5 / 66.0 / 75.9	36.1 / 42.8 / 46.3	21.4 / 29.5 / 31.3	50.6 / 54.1 / 58.8	1589.0 / 1472.0 / 1267.0
Overhang	50.5 / 63.0 / 74.0	35.0 / 42.0 / 46.2	14.0 / 25.0 / 31.1	45.9 / 44.8 / 45.2	1657.5 / 1654.5 / 1481.5
Overhang 3 sides	50.0 / 62.5 / 75.0	35.0 / 42.2 / 46.3	13.8 / 25.0 / 31.3	45.8 / 47.0 / 49.8	1660.5 / 1626.0 / 1406.5
Overhang 4 sides	50.0 / 63.0 / 75.0	35.0 / 42.0 / 46.0	13.8 / 25.0 / 31.3	45.2 / 44.7 / 46.4	1669.5 / 1636.5 / 1445.5
V-louver	41.5 / 57.5 / 66.0	29.0 / 38.0 / 43.5	6.3 / 12.5 / 18.8	45.0 / 43.0 / 42.0	/ 1671.0 / 1640.0

ASE: During the simulation process, several iterations incorrectly reported an ASE of 0% at elevated WWRs (50% and 70%). Given that the corresponding ASE values at the baseline WWR of 30% were non-zero, these outcomes were flagged as physically inconsistent. In total, 27 cases—comprising approximately 11.5% of the 234 total simulations—were identified as computational anomalies. These discrepancies are likely attributable to excessively high direct illuminance and inherent limitations within the simulation engine (Honeybee/Radiance), which can occasionally generate false zero artifacts under extreme glare conditions. To strictly maintain data integrity, these unrealistic datapoints were excised from the dataset prior to statistical analysis. Figure 6 illustrates the distribution of ASE for the baseline condition and the evaluated external shading typologies across three WWR scenarios (30%, 50%, and 70%). Across all façade configurations, median ASE exhibits a pronounced and systematic dependence on the WWR. Under the unshaded baseline condition, ASE increases monotonically with the WWR, reaching critical median values of 21.40%, 29.50%, and 31.30% at WWRs of 30%, 50%, and 70%, respectively. This substantial solar exposure at higher WWRs underscores the severe risk of direct sunlight penetration and subsequent visual discomfort in the absence of appropriate mitigation strategies.

Overhang-based shading systems—encompassing standard, three-sided, and four-sided configurations—provide only marginal reductions relative to the baseline. At a 30% WWR, the aggregated median ASE for these typologies stands at 14.00%. However, as the WWR expands to 50% and 70%, the median ASE rises sharply to 25.00% and 31.25%, respectively. The negligible performance differential compared to the unshaded baseline at high WWRs highlights the inherent limitations of standard planar and enclosed overhangs in mitigating low-angle solar ingress across expansive WWRs.

Conversely, slatted shading geometries demonstrate a substantially more robust capacity for intercepting direct solar penetration. H-louvers emerge as the most effective mitigation strategy, achieving a median ASE of merely 3.57% at the 30% WWR, and successfully capping exposure at 8.93% and 15.18% for WWRs of 50% and 70%, respectively. V-louvers exhibit a functionally similar, albeit slightly less optimal, performance profile relative to H-louvers; their median ASE values are recorded at 6.25%, 12.50%, and 18.75% across the ascending WWR scenarios.

The light shelf acts as an intermediate performer, generally underperforming slatted systems but offering measurable improvements over basic overhang configurations. The median ASE for light shelves is maintained at 12.95% at a 30% WWR, but deteriorates to 17.41% and 25.00% at WWRs of 50% and 70%, respectively.

Overall, the quantitative assessment of median ASE establishes that escalating WWRs substantially amplify the building's vulnerability to excessive sunlight. While traditional planar shading frameworks fail to maintain acceptable daylighting thresholds at extensive WWRs, highly articulated slatted systems—particularly H-louvers—provide the most resilient defense against visual discomfort in solar-intensive environments.

sDA: Figure 7 shows the variation in sDA for the unshaded baseline and six fixed shading configurations under 30%, 50%, and 70% WWRs. As anticipated, daylight sufficiency is positively correlated with the WWR; however, the rate of improvement and the statistical dispersion of the outcomes vary significantly depending on the applied shading strategy.

Under the restrictive 30% WWR scenario, daylight penetration is fundamentally limited. The unshaded baseline achieves a median sDA of 54.50%, while standard overhangs and light shelves cause marginal reductions, maintaining medians of 50.50% and 51.00%, respectively. In contrast, slatted geometries (H-louvers and V-louvers) obstruct daylight more aggressively, dropping median sufficiency to 42.50% and 41.50%. This discrepancy, alongside wider data distributions for slatted systems, highlights the vulnerability of interior spaces to daylight deficits when deeply profiled shades are paired with minimal window areas.

Increasing the WWR to 50% yields substantial improvements in interior illuminance. The baseline median sDA shifts upward to 66.00%, while overhang-based typologies and light shelves closely follow at approximately 63.00% and 64.00%, respectively. Slatted systems also exhibit significant recovery, reaching medians of 58.50% for H-louvers and 57.50% for V-louvers. This upward shift is generally accompanied by shrinking interquartile ranges, indicating a more uniform, reliable, and evenly distributed spatial daylight performance across the analyzed configurations.

Expanding the WWR further to 70% maximizes sDA across all models, yielding medians between 66.00% and 75.90%. The baseline reaches a peak of 75.90%, with light shelves closely matching this high performance at 75.00%. Standard overhangs also perform robustly, achieving a median of 74.00%. Conversely, slatted systems demonstrate lower peak values, with H-louvers and V-louvers recording medians of 67.00% and 66.00%, respectively. Despite these absolute increases, the data reveals a clear plateauing effect: the growth in sDA from 50% to 70% WWR is markedly less steep than the initial surge from 30% to 50%. This trajectory points to a threshold of diminishing returns, where excessive transparent area contributes only marginally to spatial daylight sufficiency as the perimeter zone reaches saturation.

Comparing the specific shading architectures, overhang-based systems consistently mirror the behavior of the unshaded baseline, inducing only negligible daylight penalties. Slatted systems remain highly sensitive to fenestration sizing, severely dampening sDA at lower WWRs but performing adequately at larger ratios. Notably, the light shelf emerges as an exceptionally efficient compromise; it consistently scales alongside the baseline—from 51.00% at the 30% WWR to a robust 75.00% at the 70% WWR—demonstrating its geometric capacity to facilitate deep daylight penetration without compromising sufficiency.

In summary, while enlarging the window area fundamentally drives up sDA, the specific choice of shading device dictates the ultimate efficiency of this gain. Configurations engineered for daylight redirection, particularly light shelves, offer the most robust improvements in sDA, ensuring stable daylight sufficiency across varying WWR proportions.

EUI: Figure 8 presents the distribution of annual EUI for the baseline case and fixed external shading configurations across three WWR scenarios (30%, 50%, and 70%). Results are illustrated using combined violin-box plots to report median values and the dispersion of annual energy demand.

In the unshaded baseline condition, EUI increases monotonically and significantly with WWR, confirming the dominant influence of the window area on annual energy consumption in the hot–dry climate of Mashhad. The baseline reaches peak values of 50.60, 54.10, and 58.80 kWh/m^2·year at 30%, 50%, and 70% WWR, respectively. Fixed external shading devices consistently mitigate this energy penalty, though their behavioral trends diverge significantly as WWR expands.

At a 30% WWR, median EUI values for all shaded configurations closely range between 45.00 and 46.50 kWh/m^2·year. Expanding the WWR introduces broader variations and typology-dependent trends. Overhang-based systems display non-monotonic behavior; for instance, the four-sided overhang (eggcrate) lowers the median EUI from 45.21 kWh/m^2·year at 30% WWR to 44.74 kWh/m^2·year at 50% WWR, before increasing to 46.43 kWh/m^2·year at 70% WWR. Conversely, the light shelf configuration follows the baseline's monotonic increasing trend, yielding median EUI values of 46.50, 47.00, and 48.50 kWh/m^2·year across the three respective WWR steps.

Slatted shading systems (H-louver and V-louver) demonstrate the most aggressive energy reductions and actively invert the baseline trend, yielding progressive energy reductions at elevated WWRs. At 70% WWR, V- and H-louvers achieve the lowest median EUIs of 42.00 and 42.50 kWh/m^2·year, respectively, with absolute minimums dropping as low as 36.00 kWh/m^2·year for H-louvers.

Overall, the results indicate that while enlarging the WWR substantially elevates annual energy demand in unshaded scenarios, fixed external shading devices effectively neutralize this surge. Slatted geometries prove most optimal for strict energy conservation, highlighting the critical role of integrated, climate-specific facade design in managing solar heat gains.

TCH: Figure 9 illustrates the distribution of TCH—representing the total occupied hours within the acceptable PMV range (-0.5 ≤ PMV ≤ +0.5)—for the baseline and six fixed external shading configurations across three WWR scenarios (30%, 50%, and 70%). Results are presented using combined violin-box plots to report median values and the dispersion of thermal comfort availability.
Across most facade configurations, TCH exhibits a systematic decline with increasing WWR, indicating the strong sensitivity of thermal comfort to the glazing ratio under hot–dry climatic conditions. In the unshaded baseline condition, TCH decreases monotonically from 1589 hours at 30% WWR to 1472 hours at 50% WWR, dropping significantly to 1267 hours at 70% WWR.

Fixed external shading systems effectively mitigate this thermal penalty to varying extents. Overhang-based configurations consistently improve the availability of thermal comfort relative to the baseline. For instance, standard overhangs maintain TCH values between 1606 and 1698 hours at 30% WWR, and effectively limit the drop at 70% WWR, keeping comfort hours predominantly between 1305 and 1601 hours. Among these, the four-sided overhang (eggcrate) demonstrates robust performance, maintaining peak TCH values up to 1717 hours at 30% WWR and up to 1560 hours even at 70% WWR.

In contrast, slatted shading systems (H-louver and V-louver) exhibit broader variability and unique dynamic responses to increasing glazing ratios. While some H-louvers configurations follow a downward trend (e.g., dropping to 1319 hours at 70% WWR), optimal H-louvers geometries completely reverse this penalty, achieving outstanding comfort levels that peak at 1813 hours at 70% WWR. This wide interquartile range highlights their extreme sensitivity to geometric design parameters.

Overall, the results demonstrate that while enlarging the WWR substantially compromises thermal comfort in unshaded buildings, optimized fixed external shading devices—particularly properly configured louvers and eggcrate systems—can fully neutralize this effect, underscoring the critical role of integrated facade design in hot–dry climates.

4.1. Multi-criteria comparison of shading typologies

Derived from these refined distributions of all parametric variants, Table 4 presents the median performance values for each shading category. This median-based comparison across the three examined WWRs (30%, 50%, and 70%) indicates that facade performance in the hot–dry climate is governed by the coupled interaction between glazing ratio and shading configuration, rather than by any single daylight, energy, or thermal comfort indicator.

Across all shading typologies, increasing WWR from 30% to 70% results in a systematic increase in daylight availability, as reflected by rising median values of sDA and UDI. However, this improvement in daylight sufficiency is consistently accompanied by higher ASE levels. Median ASE values increase markedly with WWR, exceeding the commonly referenced LEED threshold of 10% for several shading configurations at high glazing ratios. This trend highlights the inherent trade-off between daylight availability and the risk of overexposure in solar-intensive, clear-sky conditions.

A comparison among shading typologies reveals distinct performance patterns across the evaluated metrics. Planar shading systems, including horizontal overhangs and light shelves, generally achieve higher median sDA and UDI values at low to moderate WWR (30-50%), indicating favorable daylight availability under these conditions. Nevertheless, as WWR increases to 70%, the median ASE values associated with these systems rise substantially, accompanied by a noticeable reduction in thermal comfort availability, as reflected by declining TCH values. This suggests that planar shading geometries offer limited robustness under high-glazing conditions because of limited angular control over direct solar radiation.

Louver-based shading systems exhibit a different performance behavior. Median results indicate that H-louvers maintain comparatively moderate sDA and UDI values across all WWR scenarios, while simultaneously constraining ASE more effectively than planar shading systems. Notably, the increase in ASE with rising WWR is less pronounced for H-louvers, and the corresponding decline in TCH remains more gradual. This pattern suggests a more stable balance between daylight provision, overexposure control, and thermal comfort across varying glazing ratios.

V-louvers show a similar ability to limit direct solar exposure; however, their median UDI values are consistently lower than those of H-louvers, reflecting greater obstruction of diffuse daylight. Despite this reduction in useful daylight availability, V-louvers maintain relatively higher median TCH values at elevated WWR, indicating a stronger contribution to thermal comfort preservation under high solar loads.

Overall, the median-based multi-criteria comparison demonstrates that the selection of H-louvers was not subjective, but rather based on a constraint-driven evaluation approach. The primary prerequisite was satisfying LEED daylighting standards—specifically, maintaining sufficient sDA while effectively constraining ASE to remain as close to permissible limits as possible under extreme WWRs. While comprehensive grid-based systems (like eggcrate) provide strong protection against overexposure, they severely penalize useful daylight. Conversely, simple planar systems maintain high sDA but fail to adequately constrain ASE and cooling loads as WWR increases. H-louvers, however, successfully restrict median ASE values while preserving sufficient sDA and UDI. Among the configurations that met these baseline LEED thresholds, H-louvers demonstrated the most optimal overall performance for the south-facing facade by yielding higher UDI and TCH, while simultaneously improving EUI. This standard-compliant and balanced performance profile provides a robust, data-driven basis for selecting the H-louver typology for subsequent parametric investigation.

https://dx.doi.org/10.15627/jd.2026.30

Table 5. Performance comparison of various H-louver configurations at 50% WWR.

Shading	Depth (cm)	Spacing (cm)	sDA (%)	UDI (%)	ASE (%)	EUI (kWh/m²·year)	TCH (hr)
	10	10	60	43	8.9	41	1752
	10	15	63	43	18.0	40	1718
	20	15	59	42	7.1	42	1715
	10	20	64	43	21.4	41	1693
	20	20	62	43	8.04	39	1808
	30	20	59	42	4.46	42	1711
	10	25	63	42	23.2	42	1661
	20	25	61	43	13.4	40	1701
	30	25	62	43	6.3	41	1752

4.2. Parametric sensitivity of H-louver geometry

Following the typology-level comparison, a focused parametric examination was conducted to assess the sensitivity of H-louver performance to geometric variation. The analysis was limited to the 50% WWR scenario, representing an intermediate façade condition where trade-offs between daylight availability and solar control are most pronounced.

As summarized in Table 5, variations in louver depth and spacing produce noticeable shifts across indicators for daylight, overexposure, energy, and thermal comfort. Shallower louvers with wider spacing generally maintain higher sDA and UDI values, whereas increased depth or reduced spacing leads to progressive reductions in ASE. These reductions, however, are accompanied by corresponding decreases in daylight availability and, in some cases, marginal changes in energy demand and thermal comfort availability. Overall, the results demonstrate that H-louver performance is highly sensitive to geometric configuration, underscoring the need for geometry-level consideration when applying this shading typology under moderate glazing ratios.

To identify the optimal configuration, a strict threshold-based evaluation was applied in accordance with LEED criteria, requiring an sDA of 55% or higher and an ASE below 10%. Out of the evaluated geometries, five combinations successfully met these primary daylighting standards. Among these compliant options, the configuration with a depth of 20 cm and a spacing of 20 cm emerged as the best overall solution. It successfully balanced daylight provision (sDA of 62%, ASE of 8.04%) while simultaneously delivering the highest UDI (43%), the lowest EUI (39 kWh/m²·year), and the highest TCH (1808 hours). This indicates that this specific geometric configuration (rather than just its depth-to-spacing ratio) provides the most effective compromise between glare prevention, energy efficiency, and occupant comfort.

5. DISCUSSION

This study provides a comprehensive assessment of fixed external shading strategies under varying glazing ratios in a hot–dry, clear-sky climate. The findings reveal that façade performance is governed by nonlinear interactions between WWR and shading geometry, rather than by any single daylight, energy, or comfort indicator. The simulation results demonstrate that increasing WWR consistently enhances daylight availability, as reflected by higher sDA and UDI values, but simultaneously amplifies solar overexposure, cooling demand, and thermal discomfort. These findings reinforce prior research [10, 13, 26], suggesting that glazing optimization without integrated solar control is likely to lead to misleading performance gains in solar-intensive climates, particularly when evaluated through single-metric frameworks.

Across all shading typologies, the data indicate that the transition from 30% to 70% WWR yielded systematic increases in daylight sufficiency (approximately 20–25 percentage points in median sDA), but also led to disproportionate increases in ASE and EUI. These findings are consistent with [19, 28] and highlight the critical limitations of daylight-driven façade design approaches that prioritize spatial sufficiency metrics without explicitly accounting for overexposure risks and thermal penalties.

A comparative analysis of shading typologies shows clear performance differences. Planar shading systems, including horizontal overhangs and light shelves, maintain adequate daylight availability and acceptable UDI levels at low to moderate WWR. However, their effectiveness diminishes significantly as WWR increases; at 70% WWR, these systems exhibited elevated ASE and reduced thermal comfort hours. This diminished performance under high solar intensity and extended sun paths corroborates previous findings [22], highlighting their limited angular coverage under clear-sky conditions. A detailed breakdown of these relationships between light indices, energy consumption, and comfort levels is summarized in Figure 10.

To understand the selection of H-louvers as a highly effective typology, a comparative analysis of the inherent multi-metric trade-offs is essential. Comprehensive grid-based systems, like the four-sided overhang (eggcrate), provided the lowest ASE and relatively stable thermal comfort, but they substantially reduced useful daylight, causing spatial daylight sufficiency to drop below acceptable thresholds. Conversely, simple planar systems maintained high sDA but failed to adequately constrain ASE and

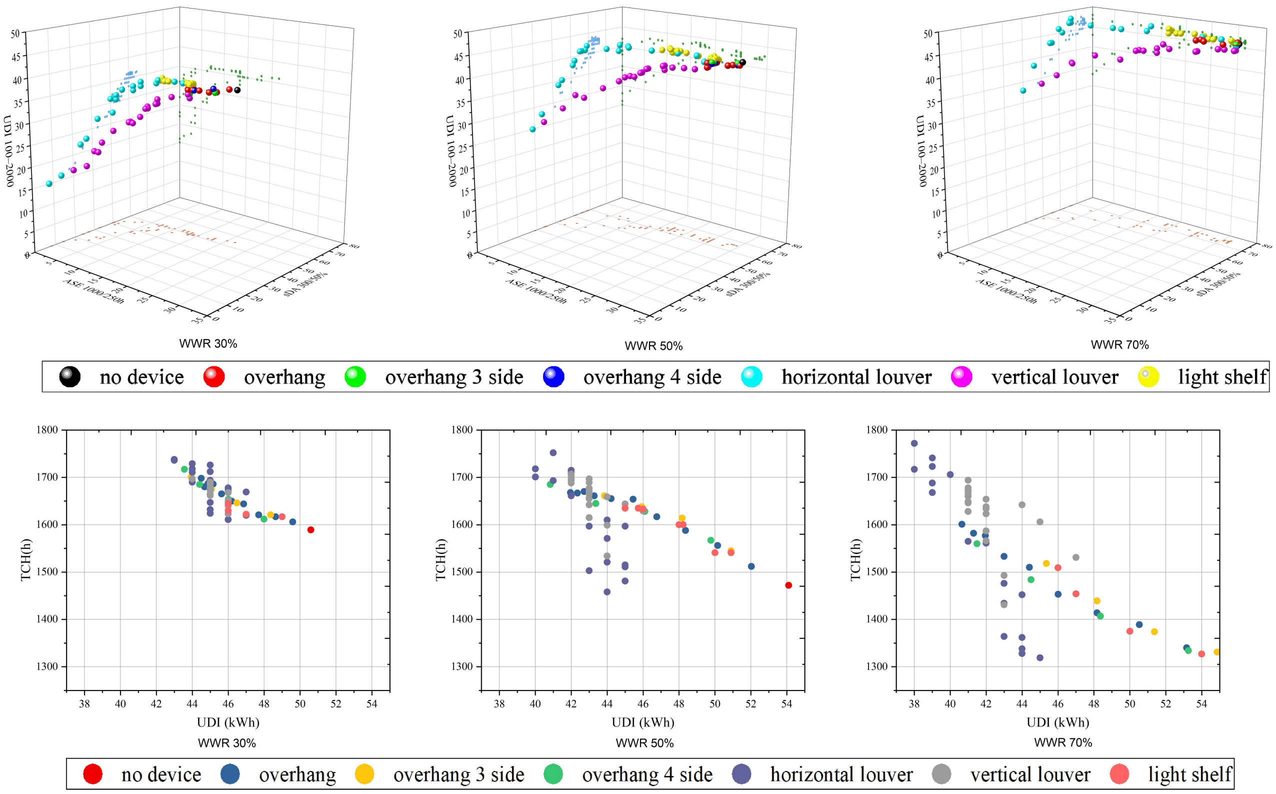

Figure 10. The relationships between light indices, energy consumption, and comfort levels.

cooling loads at higher WWRs. Therefore, H-louvers emerge as an effective Pareto-like compromise. They achieve a resilient balance through the continuous interception of direct solar radiation across a wider range of solar altitudes, restricting median ASE values near recommended thresholds while preserving sufficient sDA and UDI. While V-louvers yielded comparable control over direct sunlight, the simulations confirm observations by [25] that they tend to reduce UDI by increasing the obstruction of diffuse daylight. Consequently, H-louvers mitigate the sharp declines in thermal comfort typically seen in planar typologies as WWR increases.

The parametric analysis of H-louver geometry at 50% WWR (Table 5) employed a hierarchical evaluation to meet LEED daylight prerequisites (sDA of at least 55% and ASE of 10% or less), followed by optimizing UDI, EUI, and TCH. While shallow, widely spaced louvers failed due to excessive glare (e.g., an ASE of 23.2% at 10 cm depth and 25 cm spacing), five configurations achieved strict LEED compliance. Among these, geometries with 30 cm depth and 25 cm spacing and 20 cm depth and 20 cm spacing tied for optimal daylight availability (UDI of 43%) and energy efficiency (EUIs of 39 and 41 kWh/m²·year, respectively). However, the configuration with a 20 cm depth and 20 cm spacing emerged as the definitive optimum by maximizing thermal comfort, delivering 1808 TCH compared to the alternative's 1752 hours. These specific thresholds support the premise that shading effectiveness cannot be inferred from typology alone [31, 35] and must be rigorously optimized through a step-by-step performance evaluation.

Overall, the simulated metrics suggest that moderate glazing ratios combined with appropriately dimensioned louver-based shading systems offer a highly robust façade performance in hot–dry climates. The study supports a paradigm shift away from single-metric optimization toward integrated, multi-criteria evaluation frameworks.

While this study provides valuable insights into multi-objective façade optimization, certain methodological limitations should be acknowledged. The study employs a simplified single-zone, 6-meter-deep 'shoebox' model with adiabatic non-façade surfaces and a south-facing orientation. Although these assumptions are highly efficient for conducting a controlled parametric study, they limit the direct applicability of the findings to more complex architectural designs (e.g., deeper floor plans, multi-zone layouts) or alternative orientations. Furthermore, the simulations use deterministic standardized weather data and fixed operational schedules, which do not account for stochastic occupant behaviors (such as manual blind operation) or the impacts of future climate change. Future research could build upon these findings by integrating real-world complex architectures, dynamic shading systems, stochastic occupant modeling, and uncertainty analyses under projected climate scenarios.

6. CONCLUSION

This study investigated the multi-performance impact of six external shading typologies on a south-facing office façade in Mashhad's hot and dry climate. Through an integrated parametric simulation framework, the methodology systematically evaluated these configurations across three WWRs (30%, 50%, and 70%) to assess their combined influence on daylight availability (sDA, UDI), visual comfort (ASE), thermal comfort (TCH), and energy consumption (EUI). This comprehensive approach enabled the precise identification of performance boundaries and optimal configurations for each scenario.

The analysis confirmed that WWR is the most dominant parameter influencing the building's overall performance, and evaluating the unshaded baseline revealed the inherent conflict between daylighting and thermal/visual comfort. Quantitatively, increasing the WWR from 30% to 70% in the baseline scenario improved sDA from 54.5% to 75.9% and UDI from 36.1% to 46.3%. However, this daylighting benefit was offset by severe penalties, increasing ASE from 21.4% to 31.3% (far exceeding acceptable limits) and driving the overall EUI from 50.6 to 58.8 kWh/m^2·year. This baseline failure underscored the necessity for robust shading strategies as glazing ratios increase.

Addressing this challenge, the research identified a critical performance threshold, or "tipping point," at a WWR of 50%. Below this threshold, simpler planar systems (like overhangs) offer a viable balance of daylight access and energy savings. However, at and beyond 50% WWR, their effectiveness sharply declines, leading to significant glare and cooling penalties. In these highly-glazed scenarios, the H-louver emerged as the most effective holistic compromise. Rather than maximizing a single metric, H-louvers successfully navigated the inherent trade-offs—preventing the severe daylight penalties associated with enclosed grid systems (like eggcrates) while effectively constraining the visual glare and thermal loads that plague simpler planar systems.

Crucially, a targeted threshold-based evaluation conforming to LEED criteria (sDA ≥55% and ASE < 10%) revealed that an H-louver configuration with absolute dimensions of 20 cm depth and 20 cm spacing at a 50% WWR delivered the optimal balance among all compliant options. This specific configuration successfully mitigated the baseline penalties, achieving an ASE of 8.04%, an sDA of 62%, and a UDI of 43%, while significantly reducing the energy burden (EUI of 39 kWh/m^2·year) and maximizing thermal comfort (TCH of 1808 hours). This proves that a successful façade design strategy is not merely about selecting a shading device, but about matching its specific type and geometry to the corresponding glazing ratio.

Ultimately, this research provides architects and engineers with data-driven guidelines for designing climate-responsive facades in hot and dry environments. The identification of a clear WWR-based "tipping point" and an optimized H-louver geometry offers a practical rule-of-thumb, streamlining the decision-making process. Future work should extend this framework to other orientations and climates, incorporate more complex façade geometries, and explore the potential of kinetic systems that can adapt to changing environmental conditions.

FUNDING

This research received no external funding.

AUTHOR CONTRIBUTIONS

N.J.Y: Writing-Original Draft, Methodology, Conceptualization, Software. H.B.S: Review and Editing, Supervision, Project administration, Conceptualization, Visualization, Proofreading. M.M: Review and Editing, Visualization, Proofreading. All authors have read and agreed to the published version of the manuscript.

DECLARATION OF COMPETING INTEREST

The author declares no conflicts of interest.

REFERENCES

[1] C. Reinhart and A. Fitz, Findings from a survey on the current use of daylight simulations in building design, Energy and buildings, 38:7 (2006) 824-835.
[2] L. Heschong, R. L. Wright, and S. Okura, Daylighting impacts on human performance in school, Journal of the Illuminating Engineering Society, 31:2 (2002) 101-114.
[3] N. Nikookar, A. O. Sawyer, M. Goel, and S. Rockcastle, Investigating the Impact of Combined Daylight and Electric Light on Human Perception of Indoor Spaces, Sustainability, 16:9 (2024) 3691.
[4] C. F. Reinhart and O. Walkenhorst, Validation of dynamic RADIANCE-based daylight simulations for a test office with external blinds, Energy and buildings, 33:7 (2001) 683-697.
[5] M. L. Amundadottir, S. Rockcastle, M. S. Khanie, and M. Andersen, A human-centric approach to assess daylight in buildings for non-visual health potential, visual interest and gaze behavior, Building and Environment, 113 (2017) 5-21.
[6] A. Fang, Y. Yang, and W. Dong, Optimal design of tilted building envelope considering air conditioning energy demand, daylight utilization and glare protection-case study, Buildings, 14:2 (2024) 473.
[7] B. Givoni, Climate considerations in building and urban design, ed., John Wiley & Sons, 1998.
[8] C. Ratti, D. Raydan, and K. Steemers, Building form and environmental performance: archetypes, analysis and an arid climate, Energy and buildings, 35:1 (2003) 49-59.
[9] A. Tzempelikos and A. K. Athienitis, The impact of shading design and control on building cooling and lighting demand, Solar energy, 81:3 (2007) 369-382.
[10] M. Manzan and A. Clarich, FAST energy and daylight optimization of an office with fixed and movable shading devices, Building and Environment, 113 (2017) 175-184.
[11] C. F. Reinhart and J. Wienold, The daylighting dashboard-A simulation-based design analysis for daylit spaces, Building and environment, 46:2 (2011) 386-396.
[12] A. Nabil and J. Mardaljevic, Useful daylight illuminance: a new paradigm for assessing daylight in buildings, Lighting Research & Technology, 37:1 (2005) 41-57.
[13] C. Zheng, W. Xu, L. Wang, X. Cao, M. Li, and A. Zhang, Multi-objective optimization of energy, thermal and visual comfort for dormitory buildings in the cold climate of China, Indoor and Built Environment, 33:2 (2024) 250-268.
[14] S. Ghorbani, M. Taheri Shahraeini, and M. Mohajerani, Enhancing Daylight Performance in Educational Spaces using Light Shelves (Case Study: Architecture Studio, Shahrood University of Technology), Renewable Energy Research and Applications, 6:2 (2025) 165-178.
[15] E. Ukpong, F. O. Uzuegbunam, E. O. Ibem, and E. Udomiaye, Daylighting performance evaluation in tropical lecture rooms: A

comparative analysis of static and climate-based metrics, Journal of Building Engineering, 103 (2025) 112044.
[16] U. G. B. Council, LEED v4 for building design and construction, USGBC Inc, (2019) 85-106.
[17] K. Kalaimathy, R. S. Priya, P. Rajagopal, and C. Pradeepa, A review of daylighting calculation metrics, variables and methods in evaluating the daylight performance of a residential building, in AIP Conference Proceedings, 2023, pp. 020016.
[18] D. Esteves, J. Silva, L. Martins, J. Teixeira, and S. Teixeira, Building energy performance: comparison between EnergyPlus and other certified tools, in International Conference on Computational Science and Its Applications, 2021, pp. 493-503.
[19] B. Liu, Y. Liu, Q. Deng, and K. Hu, A study on daylighting metrics related to the subjective evaluation of daylight and visual comfort of students in China, Energy and Buildings, 287 (2023) 113001.
[20] Y. Zhou, T. Fukuda, and N. Yabuki, Automatic evaluation and analysis of indoor visual comfort for sustainable building design using interpretable ensemble learning, Automation in Construction, 181 (2026) 106582.
[21] C. Reinhart, T. Dogan, A. Jakubiec, T. Rakha, and A. Sang, UMI-an urban simulation environment for building energy use, daylighting and walkability, in Building Simulation 2013, 2013, pp. 476-483.
[22] N. Ziasistani, A. Meana-Fernández, and A. J. Gutiérrez-Trashorras, Optimization of the Performance of Double-Skin Façades Across Six Climates: Effects of Orientation, Blinds, and Overhangs on Energy Efficiency and Carbon Emissions, Thermo, 5:4 (2025) 53.
[23] L. Li, Z. Qi, Q. Ma, W. Gao, and X. Wei, Evolving multi-objective optimization framework for early-stage building design: Improving energy efficiency, daylighting, view quality, and thermal comfort, in Building Simulation, 2024, pp. 2097-2123.
[24] R. Purghorbani and H. Bagheri Sabzevar, Evaluation of Daylighting Performance, Glare Control, and Thermal Comfort Using Light Shelves and Internal Louvers in Office Buildings, Iranica Journal of Energy & Environment, 17:1 (2026) 37-51.
[25] A. A. Freewan, Impact of external shading devices on thermal and daylighting performance of offices in hot climate regions, Solar Energy, 102 (2014) 14-30.
[26] A. Maleki and N. Dehghan, Optimization of energy consumption and daylight performance in residential building regarding windows design in hot and dry climate of Isfahan, Science and Technology for the Built Environment, 27:3 (2020) 351-366.
[27] A. Martinez-Soto, G. Arias-Guerra, A. Reyes-Riveros, C. Rojas-Herrera, and D. Sanhueza-Catalán, Maximize Energy Efficiency in Homes: A Parametric Simulation Study Across Chile, Buildings, 15:21 (2025) 3828.
[28] T. Dogan and Y. C. Park, A critical review of daylighting metrics for residential architecture and a new metric for cold and temperate climates, Lighting Research & Technology, 51:2 (2019) 206-230.
[29] F. Akhlaghinezhad and H. Bagheri Sabzevar, The Effect of Probabilistic Window Opening Behavior of Occupants on Adaptive Thermal Comfort (The Case of Courtyard House in Yazd, Bandar Abbas, and Tabriz), Iranica Journal of Energy & Environment, 14:3 (2023) 252-262.
[30] L. Bellia, C. Marino, F. Minichiello, and A. Pedace, An overview on solar shading systems for buildings, Energy Procedia, 62 (2014) 309-317.
[31] F. Dokhanian, M. Mohajerani, H. Estaji, and M. Nikravan, Shading design optimization in a semi-arid region: Considering energy consumption, greenhouse gas emissions, and cost, Journal of Cleaner Production, 428 (2023) 139293.
[32] G. Dey, Daylight Optimization in Tropical Architecture: A LEED v4 Based Case Study of a Hypothetical Office Building in Chittagong, Bangladesh, (2024).
[33] L. Hong, C. Wang, and X. Zhang, Daylight Availability of Living Rooms in Dense Residential Areas under Current Planning Regulations: A Cross-Region Case Study in China, Buildings, 14:4 (2024) 1090.
[34] R. Katia and T. Rakha, Evaluating Annual Sun Exposure in LEED v4 for Commercial Office Buildings: Inclusion of Annual Glare to Enhance the Occupant Visual Performance and Comfort, LEUKOS, 21:2 (2025) 164-181.
[35] F. De Luca, A. Sepúlveda, and T. Varjas, Multi-performance optimization of static shading devices for glare, daylight, view and energy consideration, Building and Environment, 217 (2022) 109110.
[36] E. Noorzai, P. Bakmohammadi, and M. A. Garmaroudi, Optimizing daylight, energy and occupant comfort performance of classrooms with photovoltaic integrated vertical shading devices, Architectural Engineering and Design Management, 19:4 (2023) 394-418.
[37] M. Shahmoradi and M. Yeganeh, A Novel Method for Simulating Dynamic Facades to Analysing, and Optimizing Daylight and Visual Comfort in Office Buildings, Results in Engineering, (2025) 105608.
[38] M. Brzezicki, Daylight comfort performance of a vertical fin shading system: Annual simulation and experimental testing of a prototype, Buildings, 14:3 (2024) 571.
[39] D. A. Chi, Design Adjustments For Daylighting and Visual Comfort in a Classroom with Conventional Shadings, Journal of Daylighting, 11:1 (2024) 165-180.
[40] C. Pérez-Carramiñana, Á. B. González-Avilés, N. Castilla, and A. Galiano-Garrigós, Influence of Sun Shading Devices on Energy Efficiency, Thermal Comfort and Lighting Comfort in a Warm Semi-Arid Dry Mediterranean Climate, Buildings, 14:2 (2024) 556.
[41] R. Shan and L. Junghans, Multi-objective optimization for high-performance building facade design: A systematic literature review, Sustainability, 15:21 (2023) 15596.
[42] Z. Wu, Y. Xu, and Z. Wang, Multi-objective optimization of energy, view, daylight and thermal comfort for building's fenestration and shading system in hot-humid climates, PLoS One, 20:6 (2025) e0325290.
[43] A. Bahdad, S. Fadzil, H. Onubi, and S. BenLasod, Multi-dimensions optimization for optimum modifications of light-shelves parameters for daylighting and energy efficiency, International Journal of Environmental Science and Technology, 19:4 (2022) 2659-2676.
[44] E. Sorooshnia, M. Rashidi, P. Rahnamayiezekavat, F. Rezaei, and B. Samali, Optimum external shading system for counterbalancing glare probability and daylight illuminance in Sydney's residential buildings, Engineering, Construction and Architectural Management, 30:1 (2023) 296-320.
[45] F. Rezaei and A. Faraji, Performance assessment of light shelves system in office buildings, in The second internatioanl conference on art & architecture, advanced technologies, & construction management (IAAC), 2024, pp. 1-15.
[46] A. Ebrahimi-Moghadam, P. Ildarabadi, K. Aliakbari, A. Arabkoohsar, and F. Fadaee, Performance analysis of light shelves in providing visual and thermal comfort and energy savings in residential buildings, Journal of the Brazilian Society of Mechanical Sciences and Engineering, 42 (2020) 1-18.
[47] F. De Luca, J. Natanian, and T. Wortmann, Ten questions concerning environmental architectural design exploration, Building and Environment, 261 (2024) 111697.
[48] M. Mahdavinejad et al., The impact of facade geometry on visual comfort and energy consumption in an office building in different climates, Energy Reports, 11 (2024) 1-17.
[49] Y. Liu et al., Daylighting performance and thermal comfort performance analysis of west-facing external shading for school office buildings in cold and severe cold regions of China, Sustainability, 15:19 (2023) 14458.
[50] C. Reinhart, Shoeboxer: An algorithm for abstracted rapid multi-zone urban building energy model generation and simulation, (2017).
[51] C. Reinhart, A. Jakubiec, and D. Ibarra, Definition of a reference office for standardized evaluations of dynamic façade and lighting technologies, in Building Simulation 2013, 2013, pp. 3645-3652.
[52] N. B. R. o. Iran, Chapter 19: Energy Conservation, ed., Iranian National Building Regulations: Tehran, Iran, 2020, pp.